International Journal of Innovative Agriculture & Biology Research 12(1):38-52, Jan.-Mar., 2025

© SEAHI PUBLICATIONS, 2025 www.seahipublications.org ISSN: 2354- 2934

doi:10.5281/zenodo.15021831

Geospatial Analysis Of Deforestation In Falgore Game Reserve, Kano State Nigeria

***Dantani, A. and Tadda, A.H**

Department of Forestry and Wildlife Management,
Faculty of Agriculture,
Bayero University Kano, Nigeria
Correspondence: adantani.fwm@buk.edu.ng

ABSTRACT

This study titled Geospatial Analysis of Deforestation in Falgore Game Reserve, involved analysis of the spatial and temporal patterns of vegetation cover and land surface temperature (LST) from 2003-2023. The research utilized Landsat ETM+ and OLI satellite images from US Geological Survey (USGS) database, the images underwent atmospheric correction in QGIS 3.22.15 using the semi-automatic classification method. The images were obtained during dry-season to avoid vegetation overestimation; they were analyzed for vegetation cover changes using NDVI as a deforestation monitoring indicator. Vegetation cover was categorized into four classes: bare land, open woodland, shrubland, and dense forestland. Image preprocessing, including atmospheric and topographic corrections, ensured spatial comparability, while NDVI analysis in QGIS facilitated unsupervised classification. Results revealed significant vegetation cover changes, with dense forestland increasing from 31.5% to 34.4%, and open woodland expanding from 23.2% to 36.4%, while shrubland declined from 42.6% to 26.9%. Bare land fluctuated, rising to 12.8% in 2013 before decreasing to 2.3% in 2023. The LST trends showed an increase in maximum and minimum temperatures from 2003 to 2013, followed by a slight decline between 2013 and 2023. Correlation analysis between LST and NDVI indicated a weak negative relationship in 2003 (-0.3507) and 2013 (-0.1983), but stronger inverse relationship in 2023 (-0.6370), suggesting rising temperatures increasingly contributed to vegetation decline. The observed changes in vegetation were attributed to deforestation, fuelwood harvesting, grazing, and settlement expansion, highlighting ongoing land cover dynamics and climate variability in the reserve.

Keywords: Deforestation, Geospatial Analysis, Falgore Game Reserve

INTRODUCTION

Forests make up a third of the planet's landmass, covering close to 4 billion hectares (Blanc et al., 2016). The largest forested areas are located in the Boreal and Equatorial zones, this current distribution isn't fixed, but has continuously changed over time due to the influence of environmental change and human activities such as illegal logging (Kumari et al., 2020). A third of current forested areas is made up of forest that is considered primary or intact, the remaining two thirds are subject to anthropogenic activity (FAO, 2010).Forests provide a diversity of products and ecosystem services, forests also represent a reservoir of biodiversity, especially tropical forests (Blanc *et al.*, 2016). Knowing the extent of forested areas, the state of forests and how they change over time is therefore particularly important with regard to current environmental concerns that can lead to climate change such as reduction in seasonal in seasonal rainfall (Spracklen and Garcia-Carreras, 2015). Forest ecosystem modifications perpetrated profound negative impacts on sustainable food production, freshwater availability, species diversity and richness, climate, and human well-being (Overmars and Verburg, 2005). The problems of deforestation in

Nigeria's National Parks and forest reserves are largely attributed to inadequate trained staff, lack of equipment, corruption, and poor remuneration among other factors (Meduna *et al.*, 2009)

Deforestation is the complete destruction of forest cover, deforestation causes a large loss of carbon stock per unit area relative to other practices in forests (Achard *et al.*, 2010). Conversion into agricultural or pastoral land is the principal cause of deforestation, once certain areas are abandoned, forest cover can once again develop, leading to what are known as secondary forests (Blanc *et al.*, 2016). Deforestation is one of the primary sources of concern regarding climate change as it is one of the largest sources of greenhouse gas emissions in the world, second only to the burning of fossil fuels (Le Quéré *et al.*). Within the region of the Brazilian Amazon, studies have shown that deforestation, in conjunction with forest fires, can make up to 48% of the total emissions (Aragão *et al.*, 2014). It also bears substantial implications regarding the conservation of ecosystems and their biodiversity in the region, and it has been linked to the loss of species and general loss of ecosystem stability (De Bem *et al.*, 2020). Deforestation also increases surface temperature, excessive emission rates of carbon dioxide, soil degradation and increase in surface runoff resulting in flash floods. Removal of forest cover alters global and regional climate patterns and results in catastrophic rainfall spells followed by prolonged dry periods (Ali *et al.*, 2014). During the last few decades increase in urbanization and change in land use have resulted in massive increase in the rate of deforestation causing a distortion of global climate patterns and increase in catastrophic hydro-meteorological events (Winkler, 2017).

Remote sensing emerged as the only tool capable of continuously providing reliable data on the regional or continental scale (De Bem *et al.*, 2020). It involves the acquisition of information about an object, area or phenomenon through the analysis of data acquired by a device that is not in contact with the object, phenomenon or area under investigation (Kumar *et al.*, 2010). Unlike other types of land use, forests are a types of vegetations easily recognizable on satellite images (Potić *et al.*, 2023). The satellite data used to provide estimates of deforestation consist optical data, it acquired in visible and infrared wavelengths, it is sensitive to operating variables of the vegetation or chlorophyll activity (Ochego, 2003). Remote sensing, whether from aircraft or satellites, is a practical tool that provides continuous maps of vegetation changes over time, supplementing the more detailed but less synoptic ground biological surveys. It provides a means to focus remediation efforts on specific locations that need it most, instead of making wholesale changes to entire sites, and is also a valuable tool for monitoring and quantifying a wide array of biophysical changes in a particular vegetation (Borstad *et al.*, 2005; Martínez *et al.*, 2014). Normalized Difference Vegetation Index (NDVI) is commonly used in remote sensing as an index that provides a measure of green vegetative cover or biomass, measure of plant chlorophyll. Red reflectance (near 660 nm) from healthy green vegetation is low because of light absorption by photosynthetic pigments, mainly chlorophyll, whereas a plant's spongy mesophyll leaf structure creates considerable reflectance in the near infrared region of the spectrum (Peñuelas and Filella, 1998; Tucker, 1979).

Monitoring deforestation is necessary for generating valuable information for better decision making in management of forest areas (Lu *et al.*, 2003). Policies that influence the rate of converting forest to other land use or encourage afforestation and reforestation of deforested lands have the potentials to have a large impact on the vegetation and climate (Kumar *et al.*, 2010). Forests play a key role in regulating the hydrologic cycle through evapotranspiration and can be used as an effective tool to mitigate climate change, climate model simulations show that tropical forests maintain high rates of evapotranspiration, increase precipitation and results in a decrease in surface air temperature (Ali *et al.*, 2014). Forests provide social, economic, ecological and aesthetic benefits to natural systems and people. They act as a hub for biodiversity, act as food supply, have medicinal and economic value, help in hydrological cycle regulation, protect soil cover and serve as aesthetic and recreational sites. Additionally, forests influence climate through exchanges of water, carbon dioxide, energy and other chemicals with the atmosphere (Cook *et al.*, 2013). Falgore Game Reserve which is the main area of this study is facing numerous natural and human-induced causes of degradation (Badamasi *et al.*, 2010) attributed to illegal exploitation such as felling of trees for fuel, non-timber forest products' NTFPs collection such as gum arabic, honey, and medicinal plants, and uncontrolled livestock grazing by herdsmen (Dakata and Yelwa, 2012). T

The problems of Falgore Game Reserve are more profound when considered on the basis of its potential ecological services to the nation, the reserve provides a unique ecosystem that serves as an important freshwater catchment basin serving Kano, Jigawa, Bauchi, Yobe, and Borno States and Lake Chad, as well as
provision of numerous NTFPs for its proximate communities (Suleiman *et al.*, 2017). Nigeria is among the countries with the highest rate of primary forest loss the world over, with an annual average rate of 5.7% compared to the world average of 3.3% per annum, for instance, the natural forest cover in the country had decreased from 25,951 km2 in 1976 to less than 10,114 km2 in 2005, indicating a loss of about 53% of the total forestland (Millennium ecosystem assessment, 2001).

METHODOLOGY

Study area

The study was conducted in Falgore game reserve (FGR) Kano, Nigeria. The FGR formerly known as Kogin Kano Game Reserve is located between longitudes 8° 30′ and 8° 50′ East and latitudes 10° 46′ and 11° 20′ North, 150 km south of Kano city. It has an estimated area of 92,000 ha and borders Tiga artificial Lake to the north and Lame Burra Game Reserve in Bauchi State to the southeast.

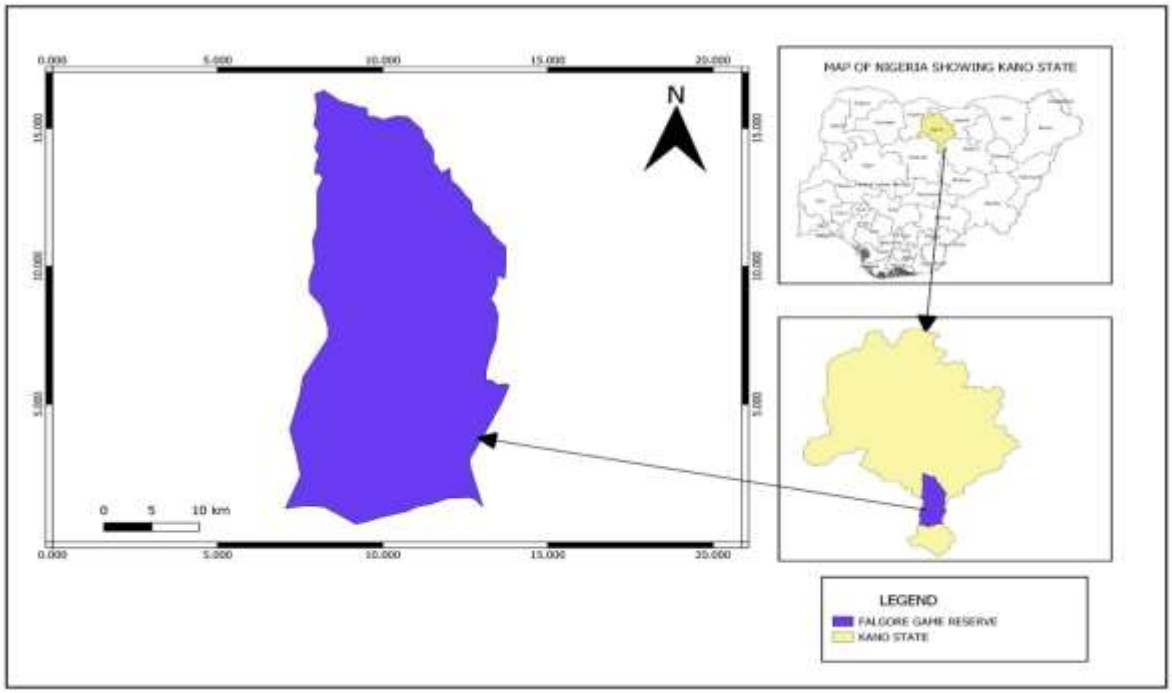

Figure 1: The Study Area

Weather and Climate

The mean annual rainfall in FGR is estimated at 1000 mm and this decreases northwards to about 800 mm around Kano Metropolitan, 700mm and high rainfall of about 4200mm in a wet year. The region is also characterized by high evaporation in the hottest months (Olofin, 2000).

Soil and Vegetation

The FGR is a gallery forest with a high density of tree species and high floristic diversity found within the open Northern Guinea Savannah woodland vegetation type, though with elements of the Sudan Savannah in the northern tip (Suleiman *et al.*, 2017). The area is characterized by rocks of the basement complex of pre-cambrian age to the west and south and the Chad formation to the northeast. The first two

geomorphological types are part of the high plains of Hausa land while the third is part of the Chad plains (Olofin, 2000).

Population

According to 2006 census figures from national population commission of Nigeria, Kano State has a population of 9,383,682 people, therefore the most populous state in the country (Eme and Idike, 2015). The annual population growth rate of the state is 3% and therefore projected to be 12,198,786 by 2016. More than a half of the inhabitants of the area are farmers involved in growing cereals, legumes, and vegetables. In addition to cultivation, livestock rearing and trade are major activities in the state. The major inhabitants of the state are the Hausa and Fulani ethnic groups whose main source of livelihoods is livestock rearing, farming, hunting, and fishing, although hunting and fishing as livelihood activities cause little or no harm to the forest ecosystem if carried out in a conventional way. (Suleiman *et al.*, 2017).

Image acquisition and Correction

The Landsat Enhanced Thematic Mapper Plus(ETM+) and the Operational Land Imager(OLI) satellite imageries for 2003,2013 and 2023 used in this study were acquired from the official website of US Geological Survey(USGS) database (http://glovis.usgs.gov/), all the images used in this study were subjected to atmospheric correction using QGIS 3.22.15 semi- automatic classification method, and also captured during the dry season to avoid overestimation of vegetation cover types (Agbor and Makinde, 2018).

Table 1: Attributes of satellite imageries. Source: USGS (http://glovis.usgs.gov/)

Satellite	Spatial resolution	Band combination	Acquisition year	Path/Row	Date
Landsat 7	30m	3,4 and 6	2003	188/52	30/04/2003
Landsat 8	30m	4,5 and 10	2013	188/52	20/06/2013
Landsat 8	30m	4,5 and 10	2013	188/52	07/06/2023

Vegetation Detection

Vegetation index reflects the approximation relation between the spectral response and vegetation cover, changes in vegetation index can reflect the changing process of land productivity. The vegetation index used as deforestation monitoring indicator to detect spatial changes of the vegetation cover. The Normalized Difference Vegetation Index (NDVI) is a simple numerical indicator that can be used to analyze remote sensing measurements from a space platform, and assess whether the target being observed contains live green vegetation or not (Kumar *et al.*, 2010)

$$NDVI = \frac{(near\ I.R - Red)}{(near\ I.R + Red)} \qquad (1)$$

Vegetation cover classification

In Nigeria, there is no standard system of vegetation cover classification for remotely sense data (Suleiman *et al.*, 2017). a classification scheme used by Wasonga (2009), and Badamasi *et al.* (2010) in their various studies for land-use and land-cover change analysis were adopted. The vegetation cover was classified into four major classes based on tree and canopy density as shown in Table 3 below.

Table 2: Classes of vegetation cover

1	**vegetation cover**	**Description**
2	Bare land	Area with no vegetation cover
3	Open woodland	Moderately scattered trees (<49%)
4	Shrubland	Area covered by shrubs (50–70%)
5	Dense forestland	Predominated by trees (>70%)

Data analysis

The acquired imageries were processed using QGIS 3.22.15. Image pre-processing including, atmospheric, and topographic corrections were carried out to ensure spatial temporal comparability of the datasets (El Haj Tahir *et al.*, 2010). The imageries were corrected and georeferenced for an effective image processing as it is a prerequisite for successful Vegetation cover change analysis (Tewolde and Cabral, 2011). All bands of the imageries used in the study were resampled to a common pixel value in order to minimize the spatial scale differences between the bands of each datasets (Suleiman *et al.*, 2017). The NDVI analysis algorithm in QGIS 3.22.15 software were used to perform an unsupervised classification of, 2003, 2013, and 2023 satellite imageries. The unsupervised classes were subsequently classified into four distinct vegetation cover classes as shown in Table 4.

Rate of vegetation change analysis

The vegetation cover change analysis was achieved by quantifying the proportion of an area occupied by a particular form of vegetation class relative to total forest area. This were followed by determination of relative changes of various vegetation classes during the stipulated period of study. The following mathematical equations were used to determine the difference between the area of various forms of the vegetation cover of the mentioned period of time under the study (Hansen *et al.*, 2013).

$$\Delta A = A2 - A1 \quad (2)$$

Where ΔA = Change area, A1 and A2 are the area of the target vegetation cover type at time 1 and time 2.

$$PAC = \frac{(\Delta A)}{(TA)} \times 100 \quad (3)$$

Where PAC = Percentage of Area Change, TA = Total Area

Annual Rate of Vegetation change = $\frac{\Delta A}{N}$ (4)

Where N is a number of years between the beginning and the end of study period.

Land Surface Temperature (LST) retrieval

To determine land surface temperature, Landsat satellite images of 2013 and 2023 were used. following recommendations of USGS on January 6, 2014 the study were not utilize TIRS Band 11 of OLI in estimating brightness temperature due to its larger calibration uncertainty(Agbor and Makinde, 2018; Avdan and Jovanovska, 2016), satellite and data were used to analyze LST variation within the study area. LST were derived from TM 6 and OLI 10 using emissivity correction model. The LST were retrieved using the following steps:

Conversion of digital numbers to atmospheric radiance

The conversion of digital numbers (DNs) of band 6 to Atmospheric radiance A_r were achieved using equation 5 (Giannini *et al.*, 2015).

$$A_r = \left(\frac{L_{max}\lambda - L_{min}\lambda}{Q_{cal}\lambda}\right) Q_{cal} + L_{min}\lambda \quad (5)$$

Where A_r is the radiance at the sensor[W/(m^2 sr µm)], Q_{cal} is the image value (Tajudin *et al.*2021), Q_{cal}min represent the minimum DN value correspond to $L_{min}\lambda$, Q_{cal}max is the maximum pixel value corresponding to $L_{max}\lambda$, $L_{min}\lambda$ is at-sensor radiance scaled to Q_{cal}min in [W/(m^2 sr µm)], $L_{max}\lambda$ is at-sensor radiance scaled to Q_{cal}max in [W/(m^2 sr µm)], in case of landsat 7, A_r were calculated using equation 6 .

$$A_r = \left(\frac{L_{max} - L_{min}}{Q_{cal}max - Q_{cal}min}\right) * (Q_{cal}\ Q_{cal}min) + L_{min} \quad (6)$$

In case of landsat 8 image, A_r were retrieved using the equation 7 (Avdan and Jovanovska, 2016)

$$A_r = mx + a \quad (7)$$

Where m is the multiplicative rescaling factor, x stands for the Band 10, and a is the additive rescaling factor.

Conversion of surface radiance to brightness temperature

After the digital numbers (DNs) converted to atmospheric radiance, the TIRS band data were converted from spectral radiance to brightness temperature (B_t) using the thermal constants that were provided in the metadata of the image. Equation 8 were used (Agbor and Makinde, 2018).

$$B_t = \left(\frac{K_2}{\left(\frac{K_1}{A_r}+1\right)}\right) - 273.15 \qquad (8)$$

Where B_t is the brightness temperature in ° Kelvin, A_r is the Atmospheric radiance, K_1 and K_2 are the thermal conversion constants that were provided in the metadata of the image. For obtaining the results in Celsius, the radiant temperature were revised by adding the absolute zero (approx. −273.15°C) (Tajudin *et al.*, 2021; Yun-hao *et al.*, 2002).

Land surface temperature emissivity estimation

Land surface emissivity(ε) is a proportionally factor that scales black body radiance (Planck's law) to predict emitted radiance. It is the efficiency of transmitting thermal energy across the surface into the atmosphere. In this sense, emissivity (ε) must be known in order to estimate LST accurately from radiance measurements. Knowledge of the emissivity spectrum is also useful for terrestrial and planetary geological studies to map surface materials based on differences in wavelength-dependent spectral features. (Agbor and Makinde, 2018).

A number of methods have been explored to estimate surface emissivity. The limitations of the different existing methods led the development of methods based on normalized difference vegetation index (NDVI) estimations from visible and near-infrared data for application to sensors without multispectral TIR capabilities. Example of such method is the NDVI thresholds method (NDVI-THM) (Avdan and Jovanovska, 2016). This method was employed in this study.

Proportion of vegetation P_v

P_v were calculated according to equation 9 (Wang *et al.*, 2015). A method for calculating P_v suggests using the NDVI values for vegetation and soil ($NDVI_v$ = 0.5 and $NDVI_s$ = 0.2) to apply in global conditions (José A Sobrino *et al.*, 2004).

$$P_v = \left(\frac{NDVI - NDVI_s}{NDVI_v + NDVI_s}\right)^2 \qquad (9)$$

Land surface emissivity (LSE) ε

The land surface emissivity(LSE(ε)) must be known in order to estimate LST, since the LSE is a proportionality factor that scales black body radiance (Planck's law) to predict emitted radiance, and it is the efficiency of transmitting thermal energy across the surface into the atmosphere (Jiménez-Muñoz *et al.*, 2006).

$$\varepsilon_\lambda = \varepsilon_{v\lambda} P_v + \varepsilon_{s\lambda}(1 - P_v) + C_\lambda \qquad (10)$$

where ε_v and ε_s are the vegetation and soil emissivities, respectively, and C represents the surface roughness (C = 0 for homogenous and flat surfaces), it will be used as a constant value of 0.004 (Sobrino and Raissouni, 2000).

When the NDVI value is less than 0, its classified as water and the emissivity value of 0.991 is assigned. For NDVI values between 0 and 0.2, it considered that the land covered with soil and the emissivity value of 0.996 is assigned. Values between 0.2 and 0.5 are considered as mixture of soil and vegetation cover. When the NDVI value is greater than 0.5, its considered to be covered with vegetation and the value of 0.973 is assigned (Avdan and Jovanovska, 2016).

The last step of retrieving the LST or the emissivity corrected land surface temperature T_s were computed using equation 11 (Stathopoulou and Cartalis, 2007).

$$T_s = \frac{B_t}{\{1 + [(\lambda B_t/\rho) In \varepsilon_\lambda]\}} \qquad (11)$$

Where T_s is the LST in Celsius, B_t is at-sensor B_t (∘C), ε_λ is the wavelength of emitted radiance (for which the peak response and the average of the limiting wavelength (λ= 10.895) will be used) (Avdan and Jovanovska, 2016; Markham and Barker, 1985),$\varepsilon\lambda$ is the emissivity calculated in (10), and$\rho = h\frac{c}{\sigma} = 1.438 \times 10^{-2} mK$ (12)

where σ is the Boltzmann constant (1.38 × 10−23 J/K), h is Planck's constant (6.626 × 10−34 Js), and c is the velocity of light(2.998 × 108 m/s)(Weng *et al.*, 2004).

RESULTS

Figure 1 presents the spatial and temporal pattern of various vegetation cover for 2003 to 2023. The spatial extent for vegetation cover classes shown in Table 4. Table 5 shows the annual rates of change of the vegetation cover types during the study period. Figure 3 presents the spatial and temporal pattern of various Land surface temperature from 2003 to 2023. Table 6 shows the Land Surface Temperature (LST) results in degrees Celsius for the years 2003, 2013, and 2023.

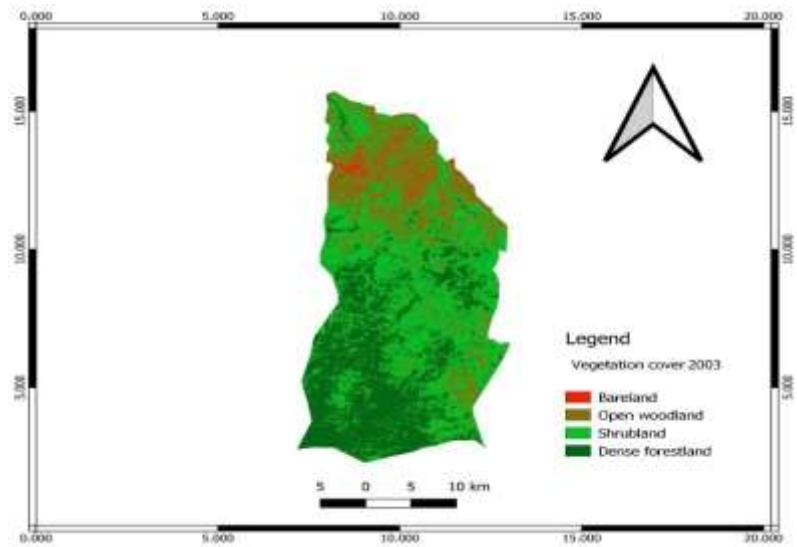

Fig. 2 1a: Vegetation cover of Falgore game reserve in 2003

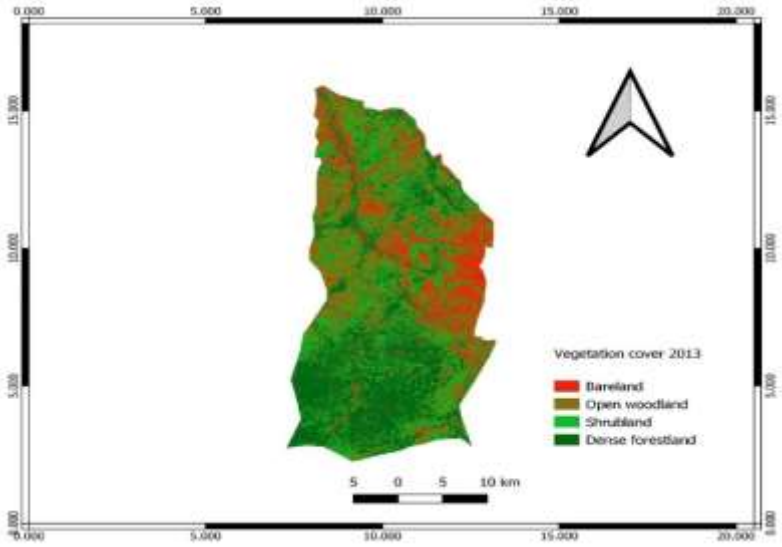

Fig. 2b: Vegetation cover of Falgore game reserve in 2013

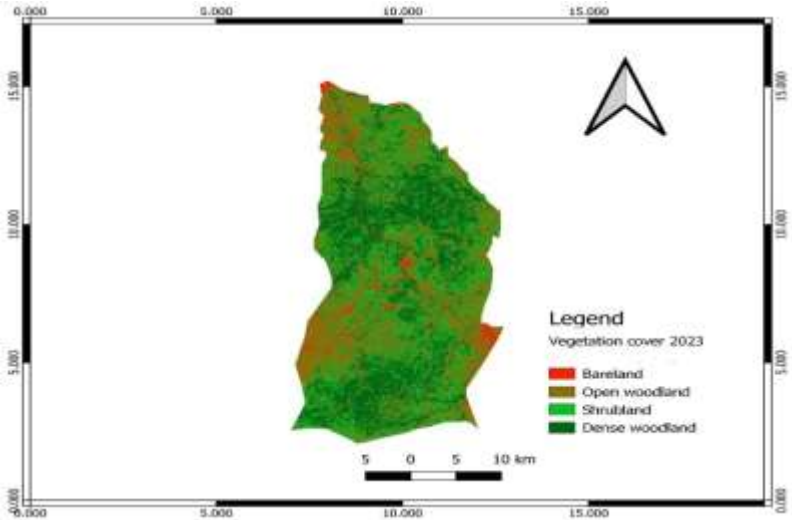

Figure 2c: Vegetation cover of Falgore game reseve in 2023

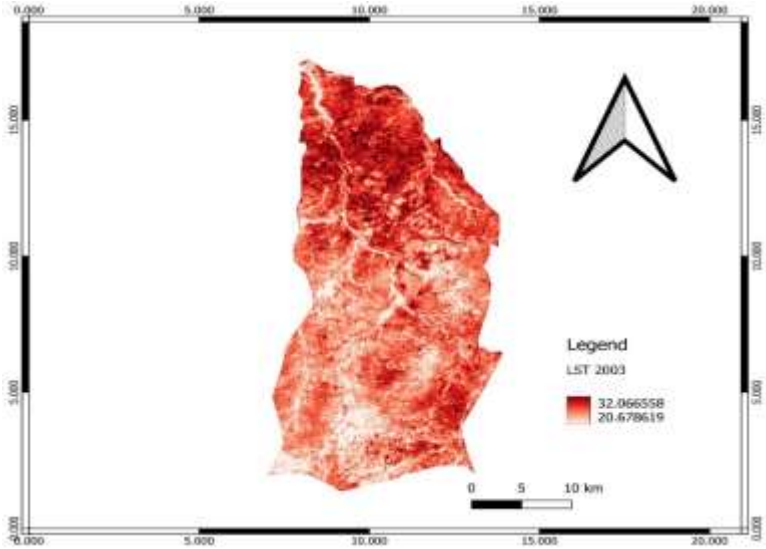

Figure 3a: Land Surface Temperature map 2003

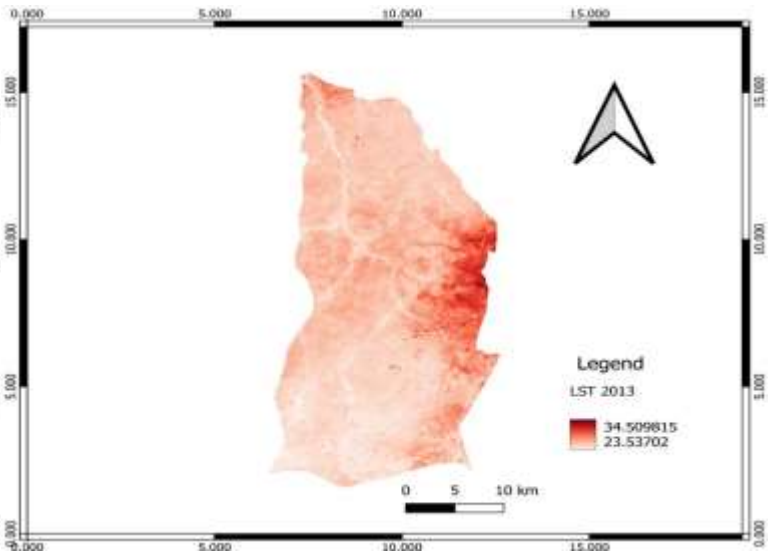

Figure 3b: Land Surface Temperature map 2013

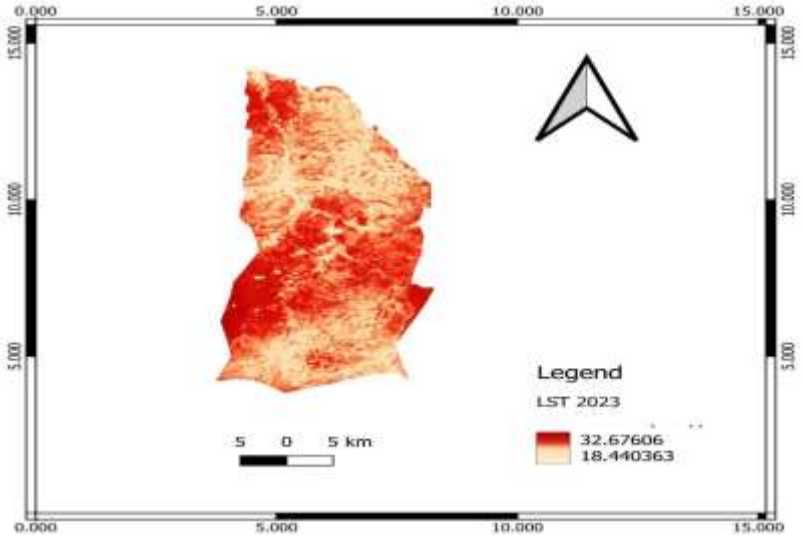

Figure 3c: Land Surface Temperature map 2023

Vegetation cover

Table 3 below revealed that; dense forestland increased from **31.5%** in 2003 to **34.4%** in 2023. Open woodland also grew, from **23.2%** in 2003 to **36.4%** in 2023. Shrubland decreased significantly from **42.6%** in 2003 to **26.9%** in 2023. Bare land saw a large shift, increasing from 2.8%) in 2003 to 12.8% in 2013, but then it decreased again to **2.3%** in 2023.

Table 3: Vegetation cover classes in Falgore game reserve during 2003-2023

Vegetation classes	**2003**	**2013**	**2023**
Dense forestland	27541.71ha (31.5%)	29502.9ha (33.7%)	30091.41ha (34.4%)
Open woodland	20329.56ha (23.2%)	25038.36ha (28.6%)	31839.12ha (36.4%)
Shrubland	37260.9ha (42.6%)	21798ha (24.9%)	23536.08ha (26.9%)
Bare land	2417.76ha (2.8%)	11210.67ha (12.8%)	2083.32ha (2.3%)
Total	**87549.9ha**	**87549.9ha**	**87549.9ha**

Changes in vegetation cover

Table 4 below presents changes in vegetation cover from 2003 to 2023, divided into two periods (2003–2013 and 2013–2023). Dense forestland increased by 2549.7 ha overall, with an annual growth of 127.5 ha (0.15%). Open woodland saw the most significant expansion, growing by 11,509.6 ha, at 575.5 ha per year (0.66%). Shrubland declined by 13,724.8 ha, shrinking by 686.2 ha annually (-0.78%). Bare land showed mixed changes, initially increasing by 8792.9 ha but then decreasing by 9127.4 ha, resulting in a minor net loss of 334.4 ha (-0.02%).

Table 4: Extent of changes in vegetation cover (2003-2023)

Vegetation cover	Changes (ha) 2003-2013	2013-2023	Overall change	Annual change	Change (%)
Dense forestland	1961.2	588.5	2549.7	127.5	0.15
Open woodland	4708.8	6800.8	11509.6	575.5	0.66
Shrubland	-15462.9	1738.1	-13724.8	-686.2	-0.78
Bare land	8792.9	-9127.4	-334.4	-16.7	-0.02

Land Surface Temperature

Table 5 below presents land surface temperature (LST) trends from 2003 to 2023: From 2003 to 2013, the maximum temperature increased from 32.07°C to 34.51°C, the minimum temperature rose from 20.68°C to 23.54°C, and the mean temperature increased from 26.38°C to 29.03°C. From 2013 to 2023, the maximum temperature slightly decreased to 32.68°C, while the minimum temperature dropped to 18.44°C, leading to a lower mean temperature of 25.56°C.

Table 5: Land Surface Temperature °C (2003-2023)

2003			**2013**			**2023**		
Max.	Min.	Mean	Max.	Min.	Mean	Max	Min.	Mean
32.07	20.68	26.375	34.51	23.54	29.025	32.68	18.44	25.56

Correlation coefficient

The table 6 shows the correlation between Land Surface Temperature (LST) and Normalized Difference Vegetation Index (NDVI) from 2003 to 2023: In 2003, the correlation coefficient was -0.3507, indicating a weak negative relationship between LST and NDVI. In 2013, the correlation weakened further to -0.1983, suggesting a very weak negative correlation. By 2023, the correlation strengthened significantly to -0.6370, showing a stronger inverse relationship between LST and NDVI.

Table 6: Correlation coefficient between LST and NDVI during 2003-2023

	2003		2013		2023	
	LST	NDVI	LST2013	NDVI	LST2023	NDVI
LST	1		1		1	
NDVI	-0.35066	1	-0.19829	1	-0.63696058	1

DISCUSSION OF THE RESULTS

Spatial and temporal pattern of various vegetation cover from 2003 to 2023.

Figure 2 presents the spatial and temporal pattern of various vegetation cover for 2003 to 2023. The spatial extent for vegetation cover classes shown in Table 2. The results reveal that Shrubland was the dominant vegetation cover type 2003, accounting for about 42.6% of the total forest area. Dense forestland was dominant in 2013 and Open woodland in 2023 covering about 33.7 and 36.4% of the reserve, respectively. Bare land occupied the least area that drastically decreased from 2.8% in 2003 to 2.3% in 2023. A corresponding decrease in area occupied by Shrubland from 42.6% in 2003 to 24.9% in 2013 is an indication that forest cover has been declining in the forest reserve. This reduction can be attributed to uncontrolled collection of non-timber forest products NTFPs, climate variability, and natural and human-induced forest fires as observed in many part of Africa (Suleiman *et al.*, 2017). The results further reveal that Bare land formed 12.8% of the total forest area of the Falgore game reserve in 2013 but sharply reduced to 2.3% in 2023. These gains were attributed to forest succession on bared land as well as natural regeneration of trees on sites where trees were cleared for fuelwood and grazing in the reserve.

The vegetation cover maps of 2003, 2013, and 2023 shown in Fig. 2 indicate that Dense forestland was predominantly along river tributaries, while open woodland was mainly found in the northern tip of the reserve where the reserve bordered Tiga artificial Lake. This could be attributed to the fact that when the lake is full, it usually submerges the northern part of the reserve thereby reducing the population densities of the trees in the affected area (Badamasi *et al.,* 2010). Figure 2c shows that the degradation trend continued and spread across the reserve as open woodland is found everywhere. These changes in vegetation cover types during this period signify a high rate of deforestation going on the reserve due to ineffective management strategies. This finding corroborates those of MEA (Millennium ecosystem assessment, 2005) that Nigeria is among the countries with the highest rate of primary forest loss the world over, with an annual average rate of 5.7% compared to the world average of 3.3% per annum, for instance, the natural forest cover in the country had decreased from 25,951 km2 in 1976 to less than 10,114 km2 in 2005, indicating a loss of about 53% of the total forestland.

Vegetation cover changes during 2003-2023

Table 4 shows the annual rates of change of the vegetation cover types during the study period. The results indicate that shrubland and open woodland have higher rate of change compared to the dense forestland and Bare land during the period of study. Between 2003 and 2023, Bare land and Shrubland decreased by 334.4 and 13724.8 ha with percentage annual change of 0.02 and 0.78%, respectively. On the other hand, dense forestland and open woodland had increased by 2549.7 and 11509.6 ha at annual rates of about 0.15 and 0.66%. Open woodland was the most dynamic during the period under study as it increased at an increasing rate. The reasons for the decrease in shrubland is partly because it is the area targeted for fuel wood and timber logging (Suleiman *et al.,* 2017). Generally, the observed increase in the extent of Vegetation cover changes during 2003 to 2023 was linked to settlement of the Fulani cattle herders in the reserve, the community fell trees to feed their livestock and construct houses. In addition, the community over relies on forest resources to meet their economic and food needs, especially at times

of scarcity, the Falgore game reserve serves as safety nets to proximate communities by offering alternative income source and food for households during the off-farming season (Yelwa, 2008).

Land surface temperature of Falgore game reserve during 2003-2023

Figure 3 presents the spatial and temporal pattern of Land surface temperature from 2003 to 2023. Table 5 shows the Land Surface Temperature (LST) results in degrees Celsius for the years 2003, 2013, and 2023. The values are classified into maximum, minimum, and mean temperatures for each respective year. The result revealed that there is an increase in both maximum and minimum temperatures from 2003 to 2013, indicating a warming trend over the period. However, between 2013 and 2023, there is slight decrease in maximum temperature and a more significant decrease in the minimum temperature. This could indicate some variability in land surface temperature over short timescales. The mean temperatures follow a similar trend as the maximum and minimum temperatures, indicating consistency in the overall land surface temperature patterns in Falgore game reserve.

Correlation between LST and NDVI

Figure 5 present the correlation between the land surface temperature (LST) and normalized difference vegetation index (NDVI) for 2003, 2013 and 2023. Table 7 shows the correlation coefficient between LST and NDVI during 2003-2023. The correlation coefficients provide insights into the relationship between LST and NDVI, which are important indicators in monitoring vegetation cover changes, particularly in the context of land cover dynamics and climate change. The result revealed that, the correlation coefficient between LST and NDVI was -0.35066 in 2003, indicating a negative correlation, these indices have been applied globally with the implicit assumption that NDVI and LST are always and everywhere negatively correlated (Karnieli *et al.*, 2019). This suggests that as LST increases, NDVI decreases, and vice versa. This negative correlation implies an inverse relationship between the land surface temperature and vegetation density. Higher temperatures may lead to decreased in vegetation density, which is reflected in lower NDVI values (Roni, 2018). Similarly, in 2013, the negative correlation continued. with a slightly lower coefficient of -0.19829. This indicates that while the negative relationship persists, it may have weakened compared to 2003. Changes in vegetation cover or climate conditions could contribute to variations in this correlation over time. In 2023, the correlation coefficient strengthened significantly to -0.63696058, indicating a stronger negative correlation between LST and NDVI compared to 2003 and 2013. This indicates that the relationship between the land surface temperature and vegetation cover became more pronounced by 2023. Several factors could contribute to this heightened correlation, such as change in vegetation cover.

CONCLUSION AND RECOMMENDATION

The study reveals significant changes in vegetation cover types over the study period. Shrubland, dense forestland, open woodland, and bare land have all experienced notable fluctuations in their spatial extents. These changes are attributed to various factors including human activities such as uncontrolled collection of non-timber forest products, climate variability, natural and human-induced forest fires. Human activities, particularly settlement and resource exploitation by the Fulani cattle herders, have played a significant role in altering the vegetation cover within Falgore game reserve. The study also revealed that the correlation analysis between land surface temperature (LST) and normalized difference vegetation index (NDVI) demonstrates a negative correlation between these variables throughout the study period. Based on the findings of this study, the following recommendations were made:

1. An alternative source of energy should be provided to reduce felling of trees for fuel wood. This would reduce over reliance on fuelwood by the local people thereby reducing the rate of destruction of natural vegetation in the area
2. Greater efforts should be directed towards restoration of degraded areas
3. More effort should be put to educate local people on sustainable and ecological procedure of harvesting medicinal herbs while encouraging them to domesticate the most commonly used tree-plants for traditional medicines to help reduced pressure on the wild stock
4. More effort should be made to involve community in the management of the game reserve

5. Public enlightenment and awareness campaign on the importance of forest and consequence of deforestation

REFERENCES

Achard, F., Stibig, H.-J., Eva, H. D., Lindquist, E. J., Bouvet, A., Arino, O., & Mayaux, P. (2010). Estimating tropical deforestation from Earth observation data. *Carbon Management, 1*(2), 271-287.

Agbor, C. F., & Makinde, E. O. (2018). Land surface temperature mapping using geoinformation techniques. *Geoinformatics FCE CTU, 17*(1), 17-32.

Ali, A., Riaz, S., & Iqbal, S. (2014). Deforestation and its impacts on climate change an overview of Pakistan. *Papers on Global Change IGBP*.

Aragão, L. E., Poulter, B., Barlow, J. B., Anderson, L. O., Malhi, Y., Saatchi, S., Phillips, O. L., & Gloor, E. (2014). Environmental change and the carbon balance of A mazonian forests. *Biological Reviews, 89*(4), 913-931.

Avdan, U., & Jovanovska, G. (2016). Algorithm for automated mapping of land surface temperature using LANDSAT 8 satellite data. *Journal of sensors, 2016*, 1-8

Babu, J. S. (2018). *Analysis and Detection of Deforestation Using Novel Remote-Sensing Technologies with Satellite Images*. Paper presented at the 2018 IADS International Conference on Computing, Communications & Data Engineering (CCODE).

Badamasi, M., Yelwa, S., AbdulRahim, M., & Noma, S. (2010). NDVI threshold classification and change detection of vegetation cover at the Falgore Game Reserve in Kano State, Nigeria. *Sokoto Journal of the social sciences, 2*(2), 174-194.

Blanc, L., Gond, V., & Minh, D. H. T. (2016). Remote sensing and measuring deforestation. In *Land Surface Remote Sensing* (pp. 27-53): Elsevier

Borstad, G. A., Martinez, M., Larratt, H. M., Kerr, R., Willis, P., & Richards, M. (2005). Using multispectral remote sensing to monitor aquatic vegetation in ponds at a reclaimed mine site.

Cook, E. R., Palmer, J. G., Ahmed, M., Woodhouse, C. A., Fenwick, P., Zafar, M. U., Wahab, M., & Khan, N. (2013). Five centuries of Upper Indus River flow from tree rings. *Journal of hydrology, 486*, 365-375.

Dakata, F. A., & Yelwa, S. A. (2012). An Assessment of Mean and Inter-seasonal Variation during Growing Season across Kano Region, Nigeria using normalized difference vegetation index derived from SPOT satellite data. *Global Advanced Research Journal of Social Sciences, 3*, 059-064.

De Bem, P. P., de Carvalho Junior, O. A., Fontes Guimarães, R., & Trancoso Gomes, R. A. (2020). Change detection of deforestation in the Brazilian Amazon using landsat data and convolutional neural networks. *Remote Sensing, 12*(6), 901.

Derbyshire, E. (1984). Quaternary glacial history of the Hunza Valley, Karakoram mountains, Pakistan. *The International Karakoram Project., 2*, 456-495.

El Haj Tahir, M., Kääb, A., & Xu, C.-Y. (2010). Identification and mapping of soil erosion areas in the Blue Nile, Eastern Sudan using multispectral ASTER and MODIS satellite data and the SRTM elevation model. *Hydrology and earth system sciences, 14*(7), 1167-1178.

FAO. (2010). Global forest resources assessment. In: Food and Agriculture Organization of the United Nations Rome, Italy.

Giannini, M., Belfiore, O., Parente, C., & Santamaria, R. (2015). Land Surface Temperature from Landsat 5 TM images: comparison of different methods using airborne thermal data. *Journal of Engineering Science & Technology Review, 8*(3).

Hansen, M. C., Potapov, P. V., Moore, R., Hancher, M., Turubanova, S. A., Tyukavina, A., Thau, D., Stehman, S. V., Goetz, S. J., & Loveland, T. R. (2013). High-resolution global maps of 21st-century forest cover change. *science, 342*(6160), 850-853.

Karnieli, A., Ohana-Levi, N., Silver, M., Paz-Kagan, T., Panov, N., Varghese, D., ... & Provenzale, A. (2019). Spatial and seasonal patterns in vegetation growth-limiting factors over Europe. *Remote Sensing*, *11*(20), 2406.

Kumar, P., Rani, M., Pandey, P., Majumdar, A., & Nathawat, M. (2010). Monitoring of deforestation and forest degradation using remote sensing and GIS: A case study of Ranchi in Jharkhand (India). *Report and opinion*, *2*(4), 14-20.

Kumari, B., Pandey, A. C., & Kumar, A. (2020). Remote Sensing approach to evaluate anthropogenic influences on Forest Cover of Palamau Tiger Reserve, Eastern India. *Ecological Processes*, *9*(1), 17. Retrieved from https://doi.org/10.1186/s13717-020-0219-z. doi:10.1186/s13717-020-0219-z

Lu, D., Moran, E., & Batistella, M. (2003). Linear mixture model applied to Amazonian vegetation classification. *Remote sensing of environment*, *87*(4), 456-469.

Markham, B. L., & Barker, J. L. (1985). Spectral characterization of the Landsat Thematic Mapper sensors. *International journal of remote sensing*, *6*(5), 697-716.

Martínez de Saavedra Álvarez, M., Brown, L. N., Lim, J. B., Ersahin, K., Borstad, G. A., Dickson, J., & Martell, P. (2014). Assessment of vegetation change after biosolids treatment: use of remotely sensed vegetation time series.

MEA (2005) Ecosystems and human well-being: synthesis. Island, Washington, DC.http://www.millenniumassessment.org/documents/document.356.aspx.pdf

Meduna, A., Ogunjinmi, A., & Onadeko, S. (2009). Biodiversity conservation problems and their implications on ecotourism in Kainji Lake National Park, Nigeria. *Journal of Sustainable Development in Africa, 10*(4), 59-73

Ochego, H. (2003). *Application of remote sensing in deforestation monitoring: a case study of the Aberdares (Kenya).* Paper presented at the 2nd FIG Regional Conference, Marrakech, Morocco.

Olofin, E. (2000). Environmental Hazards and Sustainable Agricultural Development in Northern Nigeria In: Issues in Land Administration and Development in Northern Nigeriaa. *Department of Geography, Bayero University, Kano Nigeria*.

Peñuelas, J., & Filella, I. (1998). Visible and near-infrared reflectance techniques for diagnosing plant physiological status. *Trends in plant science*, *3*(4), 151-156

Potić, I., Srdić, Z., Vakanjac, B., Bakrač, S., Đorđević, D., Banković, R., & Jovanović, J. M. (2023). Improving Forest Detection Using Machine Learning and Remote Sensing: A Case Study in Southeastern Serbia. *Applied Sciences*, *13*(14), 8289.

Roni, R. (2018). *High resolution population modeling for urban areas* (Master's thesis, University of Twente).

Sobrino, J. A., & Raissouni, N. (2000). Toward remote sensing methods for land cover dynamic monitoring: Application to Morocco. *International journal of remote sensing*, *21*(2), 353-366.

Spracklen, D., & Garcia-Carreras, L. (2015). The impact of Amazonian deforestation on Amazon basin rainfall. *Geophysical Research Letters*, *42*(21), 9546-9552.

Stathopoulou, M., & Cartalis, C. (2007). Daytime urban heat islands from Landsat ETM+ and Corine land cover data: An application to major cities in Greece. *Solar Energy*, *81*(3), 358-368.

Suleiman, M. S., Wasonga, O. V., Mbau, J. S., & Elhadi, Y. A. (2017). Spatial and temporal analysis of forest cover change in Falgore Game Reserve in Kano, Nigeria. *Ecological Processes*, *6*(1), 1-13.

Tajudin, N., Ya'acob, N., Ali, D. M., & Adnan, N. A. (2021). Soil moisture index estimation from Landsat 8 images for prediction and monitoring landslide occurrences in Ulu Kelang, Selangor, Malaysia. *International Journal of Electrical and Computer Engineering (IJECE), 11*(3), 2101-2108.

Tewolde MG, Cabral P (2011) Urban sprawl analysis and modeling in Asmara, Eritrea. Rem Sens 3:2148–2165

Tucker, C. J. (1979). Red and photographic infrared linear combinations for monitoring vegetation. *Remote Sensing of environment*, *8*(2), 127-150.

Wang, F., Qin, Z., Song, C., Tu, L., Karnieli, A., & Zhao, S. (2015). An improved mono-window algorithm for land surface temperature retrieval from Landsat 8 thermal infrared sensor data.*Remote Sensing,7*(4),4268-4289.

Weng, Q., Lu, D., & Schubring, J. (2004). Estimation of land surface temperature–vegetation abundance relationship for urban heat island studies. *Remote Sensing of environment, 89*(4), 467-483.

Winkler, H. (2017). Introduction: Emerging lessons on designing and implementing mitigation actions in five developing countries. In *Climate Change Mitigation Actions in Five Developing Countries* (pp. 9-11): Routledge.

Yelwa,(2008) Broad scale Vegetation Change Assessment across Nigeria from Coarse Spatial and High Temporal Resolution, A VHRR Data. Cuvillier Verlag, Gottingen, p 350

Yun-hao, C., Jie, W., & Xiao-bing, L. (2002). A study on urban thermal field in summer based on satellite remote sensing. *Remote Sensing for Natural Resources, 14*(4), 55-59.